Dalton Transactions

Evaluating the Photophysical and Photochemical Characteristics of Green-Emitting Cerium(III) Mono-Cyclooctatetraenide Complexes

Journal:	*Dalton Transactions*
Manuscript ID	DT-ART-02-2023-000351.R1
Article Type:	Paper
Date Submitted by the Author:	31-Mar-2023
Complete List of Authors:	Pandey, Pragati; University of Pennsylvania, Chemistry Yang, Qiaomu; University of Pennsylvania, Gau, Michael; University of Pennsylvania, Department of Chemistry Schelter, Eric; University of Pennsylvania, Chemistry

Evaluating the Photophysical and Photochemical Characteristics of Green-Emitting Cerium(III) Mono-Cyclooctatetraenide Complexes

Pragati Pandey,[a] Qiaomu Yang,[a] Michael R. Gau,[a] and Eric J. Schelter*[a]

[a] P. Roy and Diana T. Vagelos Laboratories, Department of Chemistry, University of Pennsylvania, 231 South 34 Street, Philadelphia, Pennsylvania 19104, United States

Abstract: The photophysical and photochemical reactivity of the organometallic *mono*(cyclooctatetraenyl)-Ce(III) complexes: $[(C_8H_8)Ce(\mu\text{-}X)(THF)_2]_2$ X = $O_3SCF_3^-$ (**1**), Cl^- (**2**), were studied. In the course of these studies, a new polymorph of $[(C_8H_8)Ce(\mu\text{-}O_3SCF_3)(THF)_2]_2$ (**1**) was described. Photoluminescence (PL) studies of **1** and **2** showed characteristic excitation and emission bands in the visible region, with bright green light emission under light irradiation from states corresponding to the 5d→4f transition. Complexes **1** and **2** exhibit relatively long lifetime of 205.4± 0.2 and 145.8 ± 0.4 ns respectively. And the quantum yields (Φ) for **1** and **2** are 0.180 and 0.068 respectively. Electrochemical studies were performed on complexes **1** and **2** with a reversible Ce(III)/Ce(IV) redox couple recorded at $E_{1/2}$ = −1.53 V versus the Fc/Fc^+ for **2**. Complex **1** shows an irreversible Ce(III/IV) oxidation wave. Complexes **1** and **2** revealed strongly-reducing, estimated, excited state reduction potentials ($E_{1/2}$*) of −3.31 and −4.02 V versus the Fc/Fc^+ respectively, with small Stokes shifts of 0.12 eV. With their associated relatively long lifetimes, small Stokes shifts and large, negative $E_{1/2}$* values, both complexes were evaluated as potential photosensitisers for halogen atom transfer (XAT) using a test reaction of the dehalogenation of benzyl chloride.

Introduction:

The chemistry of the cyclooctatetraenide anion ($C_8H_8^{2-}$) has been developed extensively in f-element chemistry,[1, 2] as well as being important historically in f-block chemistry with the discovery and study of uranocene, $U(C_8H_8)_2$.[3-5] Recent studies of the dianion have included those on in single ion magnet (SIM) systems with rare earth metals cations such as Dy(III) and Er(III).[6] Another important example is cerocene: $Ce(C_8H_8)_2$, a compound with a multi-configurational ground state that has been compared to a zero-dimensional, molecular Kondo system.[7, 8] In terms of synthetic chemistry, dimeric *mono*(cyclooctatetraenide)lanthanide(III) halides of the type: $[(C_8H_8)Ln(\mu\text{-}Cl)(THF)_2]_2$ Ln = Ce, Pr, Nd, and Sm are the most important precursors due to their labile bridging ligands. The synthesis of these *mono*(COT)-organolanthanide complexes were initially reported by Streitwieser in 1972.[9-11] Due to the poor solubility of the cerium(III) congener: $[(C_8H_8)Ce(\mu\text{-}Cl)(THF)_2]_2$ in the polar aprotic solvent THF, another precursor with bridging triflate ligands $[(C_8H_8)Ce(\mu\text{-}O_3SCF_3)(THF)_2]_2$ was synthesized by Edelmann.[12] These organometallic complexes have not been studied outside of their application as synthetic precursors.

Among the lanthanides, cerium(III) complexes and materials exhibit unique photophysical properties due to accessible, parity-allowed 4f-5d transitions. Moreover, the 5d ligand field states can be modulated by the coordination environment at the metal complex to tune the emission wavelength and brightness. These characteristics are unlike other rare earth metal cations, *e.g.* Eu(III) and Tb(III), that exhibit forbidden f-f transitions that are not strongly influenced by their coordination environment. The application of these photophysical characteristics of cerium(III) complexes in photoredox chemistry is also of interest owing to the comparable crustal abundance of cerium to metals such as copper[13], and the position of cerium as a waste by-product from the separation of light rare earth metals.

Initial studies on the photophysical properties of the cerium organometallic complexes including: $Cp_3Ce(THF)$, $(C_5Me_5)CeI_2(THF)_3$, $[Li(THF)_4][CePh_4]$, $[Li(tmeda)]_3[CeMe_6]$, $[K(diglyme)][(COT)_2Ce]$, $CeCl_3(THF)_x$, and $CeI_3(THF)_x$) were reported by the Bruno and Hazin in 1987 in studies of metal-ligand bond covalency.[14] However, the lifetimes, quantum yields, and photoinduced redox properties of the compounds were not disclosed. Recently, Edelmann and co-workers also used

photoluminescence as a means to support assignment of the oxidation state of Ce in the organocerium complex [{(1,3-^{t}Bu$_2$-C$_5$H$_3$)$_2$Ce(μ-Cl)}$_2$].[15]

In recent years our group has performed photophysical and mechanistic studies on the photoinduced redox properties of cerium complexes.[16-22] For the current work, we were interested to extend our studies to cerium(III) complexes comprising hydrocarbyl ligands. In the course of preparing the reported organometallic *mono*(cyclooctatetraenyl)-Ce(III) complexes ([(C$_8$H$_8$)Ce(μ-X)(THF)$_2$]$_2$, X = O$_3$SCF$_3^-$, (OTf$^-$) (**1**), Cl$^-$ (**2**), we noted that these compounds exhibited strong, RT luminescence that warranted further study. Herein, we report the photophysical data for these COT^{2-} complexes, the impact of the different bridging ligands –O$_3$SCF$_3$, –Cl on the photophysical properties of **1** and **2**, and the potential of such compounds to act as photosensitizers through dehalogenation reaction of benzyl chloride.

Result and Discussion

Synthesis and Characterization

The dimeric *mono*(cyclooctatetraenyl)-Ce(III) complexes with triflate (–O$_3$SCF$_3$) and chloride (–Cl) were synthesized with modifications of their literature procedures.[9, 11, 12] Reaction of equimolar ratios of anhydrous Ce(O$_3$SCF$_3$)$_3$ or solvated CeCl$_3$(THF)$_{1.5}$ with K$_2$C$_8$H$_8$ in the tetrahydrofuran (THF) resulted in the complexes: [(C$_8$H$_8$)Ce(μ-O$_3$SCF$_3$)(THF)$_2$]$_2$ (**1**) and [(C$_8$H$_8$)Ce(μ-Cl)(THF)$_2$]$_2$ (**2**) respectively (Scheme 1). Purification of the complexes **1** and **2** were carried out without using the reported Soxhlet extraction at the expense of reductions in yield from 62% to 58% for **1** and 30–60% to 52% for **2** (details are provided in the experimental section). Despite the reductions in yield, especially for **2**, we found the modified procedure to be for convenient to generate synthetic quantities of **1** and **2** for further studies.

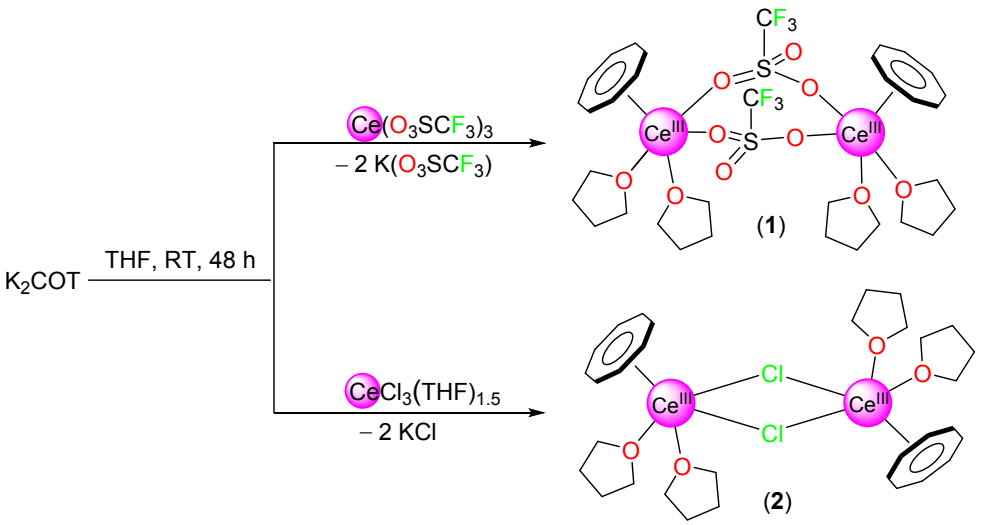

Scheme 1. Synthesis of *mono*(cyclooctatetraenyl)-Ce(III) complexes **1** and **2**.

Notably, the unit cell parameters obtained from indexing crystals grown from slow cooling of a saturated solution of **1** in THF/hexanes and a saturated THF solution of **2**, both at –20 °C, did not match with the previous reported cell parameters.[9, 23] In the case of **1**, the molecular structure revealed a polymorph that crystallized in the monoclinic $P2_1/c$ space group, different from the reported triclinic $P\bar{1}$ space group. A potential cause for isolation of the new polymorph of **1** is in the purification step. Compound **1** was purified at lower temperature using a cold THF extraction rather than using a reported Soxhlet extraction with refluxing THF. We tentatively ascribe the *cisoid* confirmation of triflate groups in **1** to this lower temperature process, as compared to the higher temperature *transoid* isomer isolated previously. In the new polymorph of **1**, each Ce cation is eight-coordinate with η^8-$C_8H_8^{2-}$ ligands and the coordination sphere is completed with THF molecules and bridging, bidentate triflate groups (Figure 1). The central eight-member ring, consisting of the $Ce_2O_4S_2$ atoms, *i.e.* Ce(1)–O(1)–S(1)–O(2)–Ce(2)–O(5)–S(2)–O(4)–Ce(1), is not planar. The Ce–O–S angles differ from each other within the new structure: Ce(1)–O(1)–S(1) 164.1(1)°, Ce(1)–O(4)–S(2) 159.4(1)°, but in comparison to the previously reported structure: Ce–O–S(1) 161.4°, Ce–O–S(2) 143.6°, the eight-member ring is less distorted (see Table 1 for comparison). Although the molecular structure is dimeric in the new space group as before, the most notable difference between the polymorphs was found in the orientation of bridging triflate groups and the central eight-member ring (Scheme 2). In comparison to the reported structure by Edelmann,[23] the $-CF_3$ groups of the bridging triflate moieties are axially proximate to one another. And the distance between the two $-CF_3$ groups C(1)–C(2) = 5.127 Å, which is shorter than in the reported structure: C(9)–C(10) = 6.626 Å. The deviation between the Ce–O–S angles between the structures (Ce(1)–O(1)–S(1) 164.1(1)°, Ce(1)–O(4)–S(2) 159.4(1)° is less (4.7°) compared to the reported structure (Ce–O–S(1) 161.4°, Ce–O–S(2) 143.6°) where the deviation was 17.8°. The Ce–$C_8H_{8(centroid)}$ distances are 1.993–1.997 Å in the new structure, which are similar to the previously reported ones by Edelmann. The

Ce–O_{THF} distances (2.570(2)–2.583(2) Å) are identical to the literature report (see Table 1 for comparison).

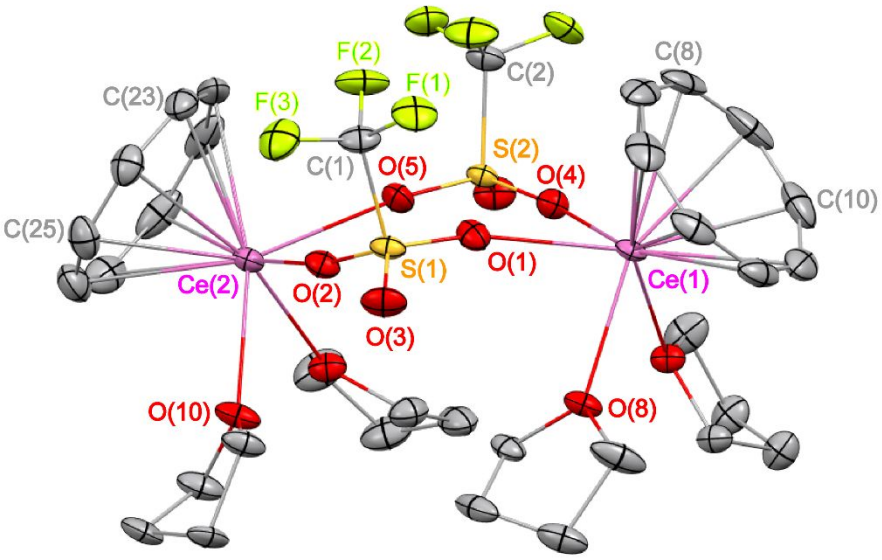

Figure 1. Molecular structure of **1** with important atoms labelled. All hydrogen atoms are omitted for the sake of clarity. Thermal ellipsoids are drawn at the 30% probability level. Selected bond lengths (Å) and angles (°): Ce(1)−O(1): 2.512(2), Ce(1)−O(4): 2.706(3), Ce(1)−O(8): 2.5761(19), Ce(2)−O(2): 2.517(2), Ce(2)−O(5): 2.511(2), Ce(2)−O(10): 2.584(2), C1(1)−S(1): 1.821(3), C(2)−S(2): 1.822(3), O(5)−S(2): 1.443(2), O(6)−S(2): 1.418(2), C(1)−F(1): 1.321(4), C(1)−F(2): 1.331(4), C(1)−F(3): 1.337(4). O(1)−Ce(1)−O(4): 73.40(7), O(2)−Ce(2)−O(5): 73.71(7), Ce(1)−O(1)−S(1): 164.13(14), Ce(2)−O(2)−S(1): 158.36(13), S(2)−O(5)−Ce(2): 164.21(14), S(2)−O(4)−Ce(1): 159.35(13).

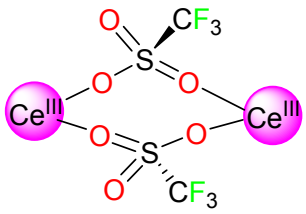

Reported structure
Triclinic P-1

Ce–O–S angles deviation
17.8°

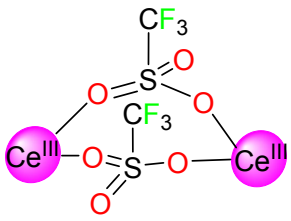

This work **1**
Monoclinic P21/c

Ce–O–S angles deviation
4.7°

Scheme 2. Two polymorphs of $[(C_8H_8)Ce(\mu\text{-}O_3SCF_3)(THF)_2]_2$ with central eight member rings comprising $Ce_2O_4S_2$ atoms.

Table 1 Selected bond length (Å) and bond angles (°) for complex $[(C_8H_8)Ce(\mu\text{-}O_3SCF_3)(THF)_2]_2$ in reported structure and new polymorph (**1**).

Reported Structure	**1**
C(9)−F(1): 1.319(5)	C(1)−F(1): 1.321(4)
C(9)−F(2): 1.312(4)	C(1)−F(2): 1.331(4)
C(9)−F(3): 1.328(5)	C(1)−F(3): 1.337(4)
C(9)–C(10): 6.626	C(1)–C(2): 5.127
Ce(1)−O(1)−S(1): 160.68(1)	Ce(1)−O(1)−S(1): 164.13(14)
Ce(1)−O(3)−S(2): 149.6(2)	Ce(1)−O(4)−S(2): 159.35(13)
Ce(2)−O(4)−S(2): 137.6(2)	Ce(2)−O(2)−S(1): 158.36(13)
Ce(2)−O(2)−S(1): 162.1(2)	Ce(2)−O(5)−S(2): 164.21(14)
O(7)–Ce(1)–O(8): 68.60(8)	O(7)–Ce(1)–O(8): 70.50(7)
O(9)–Ce(2)–O(10): 70.96(1)	O(9)–Ce(2)–O(10): 70.02(7)
$Ce–C_8H_{8(centroid)}$: 1.983–1.985	$Ce–C_8H_{8(centroid)}$: 1.993–1.997
$Ce–O_{THF}$: 2.556(2)–2.592(2)	$Ce–O_{THF}$: 2.570(2)–2.583(2)

For the dimeric complex: $[(C_8H_8)Ce(\mu\text{-}Cl)(THF)_2]_2$ (**2**) although the unit cell parameters are different from the previous report, and evidently represent a new crystalline polymorph of the compound, the gross structure, obtained from an initial solution for this polymorph, is essentially identical to the reported structure.[9, 11] Details of the unit cell parameters for the new polymorphs of **1** and **2** are provided as Supporting Information. ^{1}H-NMR spectroscopy, FT-IR spectroscopy, and elemental analysis of complexes **1** and **2** were found to be identical to the literature reports. IR data for **1** and **2** were found to be slightly different than the reported polymorphs and a comparison of the IR data with the reported ones are included as supporting information. Having established simplified synthesis and the new polymorphs of **1** and **2**, we next turned toward studies of their photoluminescence and photoredox properties.

Photophysical Studies

Solution phase UV-vis electronic absorption studies and luminescence studies were carried out to investigate the photophysical properties of **1** and **2**. The UV-vis absorption spectra for the greenish yellow THF solutions of **1** and **2** are shown in Figure 2. The absorption maxima for **1** was observed at 472 nm and for **2** at 477 nm, similar to the literature report,[10] with broad absorptions present in range of 325–375 nm. The lower energy absorptions with maxima at 472 (**1**) and 477 (**2**) nm were assigned to the two 4f–5d transitions of the Ce(III) cations, from the $^2F_{5/2}$ ground state, which are in good agreement with other reported Ce(III) complexes.[17, 21, 24, 25] It is notable that the absorption energies for complexes **1** and **2** are so similar. The most notable difference between them in the absorption spectra is that a shoulder on the 477 nm peak for **2** (assigned to the higher energy $^2F_{5/2}\rightarrow{}^2D$ transition) is better resolved than that observed for **1**. These results indicate that the bridging X-ligands have little effect on the absorption energies and that the essential electronic structure can be largely attributed to the $[(COT)Ce^{III}]^+$ interaction. The trailing intensity at higher energies in these spectra is tentatively assigned to COT^{2-} ligand-based transitions.

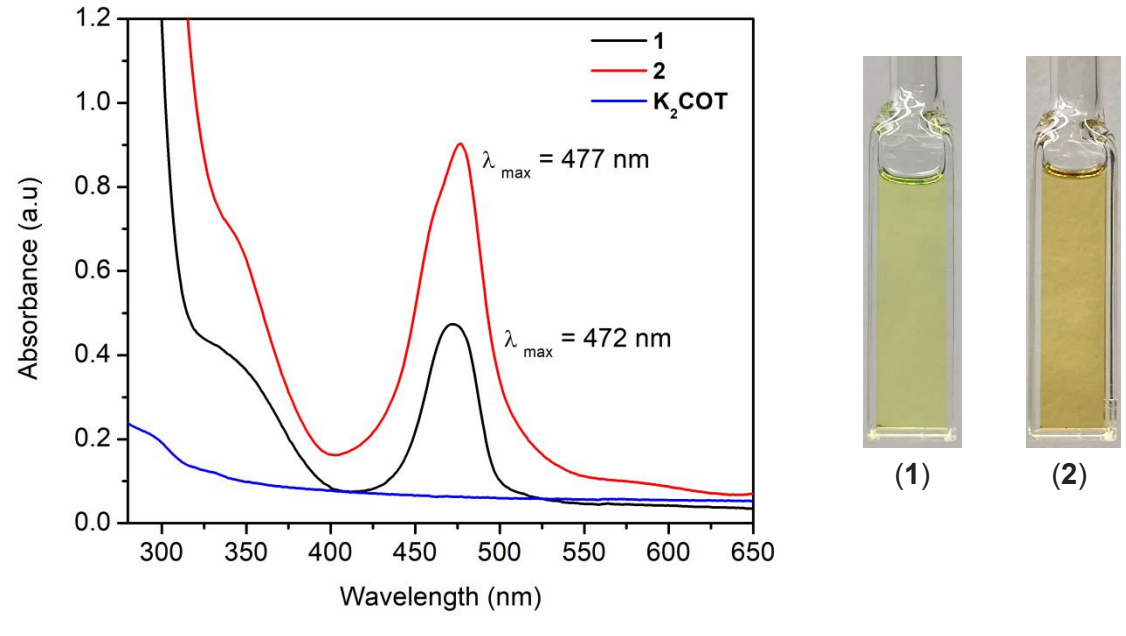

Figure 2. UV-Vis electronic absorption spectra of complexes **1** (0.5 mM), **2** (~0.7 mM) and **K_2COT** (0.12 mM) in THF.

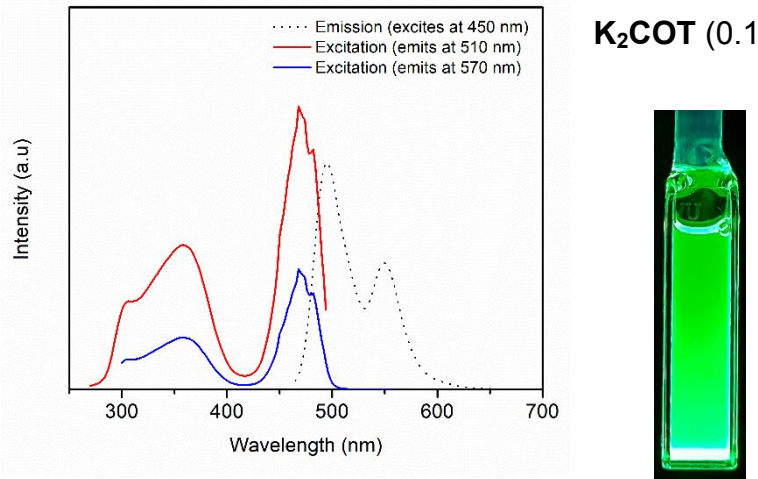

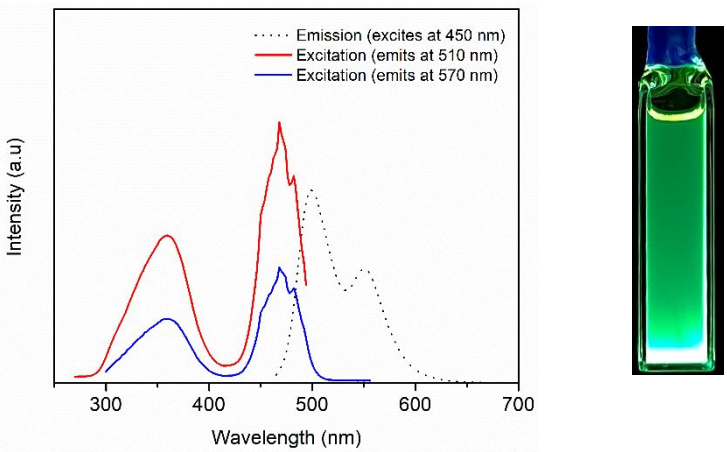

Figure 3. Photoluminescence spectra of **1** (0.5 mM) (top) and **2** (~0.7 mM) (bottom) in THF solutions, including emission spectra at 450 nm excitation (black dash), excitation spectra (red) at 510 nm emission, and excitation spectra (blue) at 570 nm emission. Images of THF solutions of **1** and **2** in 1 cm path length quartz cuvettes (~1.0 mM) under short wavelength UV irradiation (right).

The two complexes also showed emission- and excitation-spectra in THF that were similar between them (Figure 3). Upon excitation at 450 nm, two characteristic emission bands at λ_{em} = 495, 549 nm and 499, 551 nm are observed for complexes **1** and **2** respectively, due to cerium(III)-based 5d→4f emission from the excited state (^{2}D) to the ground states: $^2F_{5/2}$ and $^2F_{7/2}$ (Figure 3). Both complexes exhibit bright green emission under UV irradiation. The energy difference between the peaks in the

emission spectra is 1987 and 1891 cm^{-1} for **1** and **2** respectively, which is in agreement with the energy splitting of two 4f ground levels $^2F_{5/2}$ and $^2F_{7/2}$.[26, 27] The excitation spectra for **1** and **2** are observed in the range of 300 to 500 nm. To support assignment of the dimeric speciation of **1** and **2** in THF solution, solid-state photoluminescence spectra of the complexes were also recorded. In these cases, similar characteristic features were observed in the solid state excitation and emission spectra compared to those observed from THF solutions. Emission bands at λ_{em} = 498, 533 nm of almost equal intensity are observed for complex **1** in the solid state measurement (Figure S10), similar to the solution emission bands at 495 and 549 nm. For complex **2**, the higher energy emission band was not well resolved, comprising a shoulder at ~515 nm, associated with a more intense band at 550 nm (Figure S10). Nevertheless, the energies of these bands compared well to the solution emission bands at 499, 551 nm for **2**. Overall, the solid state PL measurements suggest that the dimeric speciation of **1** and **2** are maintained solution under these conditions, as judged by comparisons of the similar energies of the two 5d→4f emission bands in both cases. Moreover, the different band intensities between the solution and solid state measurements presumably correspond to different non-radiative decay pathways from the associated excited states under the solid state versus solution conditions.

The solution phase emission bands of colourless $Ce(CF_3SO_3)_3$, measured in EtOH, and colourless $CeCl_3(THF)_3$, measured in THF, have been reported in the UV region ~350–360 nm.[14, 26] Coordination of the $C_8H_8^{2-}$ ligand to the Ce(III) ions evidently results in a red shift of the absorption bands into the visible range at 477 and 472 nm, due to increased crystal field splitting of the 5d-manifold. The associated emission maxima for **1** and **2** are at ~500 nm. Our previous studies of series of cerium(III) emitters indicated that vibrational losses in the ^2D excited state, presumably due to the $C_8H_8^{2-}$ ligands in the current case, were correlated with the magnitude of the Stokes shifts.[16, 17, 19, 21] The Stokes shifts determined for complexes **1** and **2** are similar, with values of 0.12 eV (23 nm) (Figure S6-S7 and Table S4), a remarkably smaller value than that for our previously reported Ce(III) complexes.[19] These data indicate the complexes undergo only small vibrational relaxations of their electronic excited states. Further, with small Stokes shifts values, we expected these complexes could be used as effective photo-reductants, due to only small energy losses in the excited state.

To collect for information on the potential for **1** and **2** to act as photoreductants, lifetimes (τ) of the excited states for **1** and **2** were measured (Figure 4). Notably, for complex **1** the measured lifetime was 205.4± 0.2 ns, which is one of the longest lifetimes reported for Ce(III) complexes. Our group previously reported a guanidinate Ce(III) complex $[(Me_3Si)_2NC(N^iPr)_2]_2Ce(N(SiMe_3)^tBu)$ with a comparable lifetime of 221 ns.[21] The lifetime of the excited state of **2** is 145.8 ± 0.4 ns, which is comparatively less than **1**, but still longer than other reported Ce(III) complexes (Table 2).[17, 18]

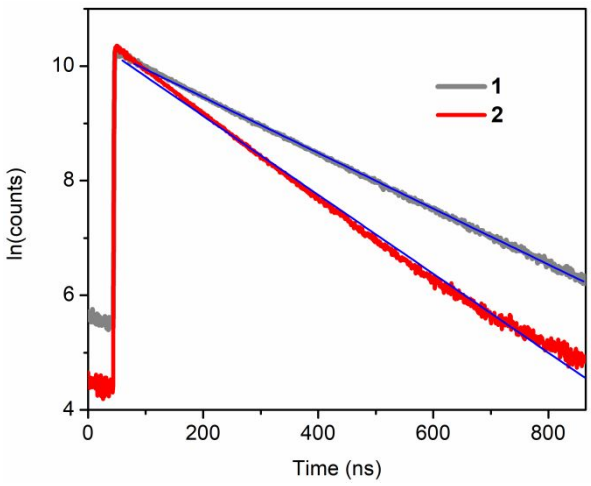

Figure 4. The ln(counts) versus time plot of time-resolved emission intensity decay for **1** (gray) and **2** (red) in THF. A fit for each complex is given with blue lines, affording τ = 205.4± 0.2 ns for **1**, and τ = 145.8 ± 0.4 ns for **2**.

Table 2: Comparison of lifetime (τ) (ns) of **1** and **2** with Ce(III) emitters reported in litertaure[17-19, 21, 24, 25]

Ce(III) Emitters	**Lifetime (τ) (ns)**
$Ce[N(SiMe_3)_2]_3$	24
$[(Me_3Si)_2NC(N^iPr)_2]Ce[N(SiMe_3)_2]_2$	65
$[(Me_3Si)_2NC(N^iPr)_2]_2Ce[N(SiMe_3)_2]$	117
$[(Me_3Si)_2NC(N^iPr)_2]_3Ce$	83
$[(Me_3Si)_2NC(N^iPr)_2]_2Ce(N(SiMe_3)^tBu)$	221
$[(Me_3Si)_2NC(N^iPr)_2]_2Ce(N(SiMe_3)^iPr)$	158
$[(Me_3Si)_2NC(N^iPr)_2]_2Ce(NPh^iPr)$	41

$[(Me_3Si)_2NC(N^iPr)_2]_2Ce(NPh_2)$	43
$[Ce^{III}Cl_6]^{3-}$	22.1
Ce-1Tp^{Me}-OTf[24]	45
Ce-2Tp^{Me2}-OTf[24]	54
$Ce(Tp^{Me2})_2$(dppz)[25]	124
1	205.4± 0.2
2	145.8 ± 0.4
Tp^{Me} = hydrotris(3-methylpyrazolyl)borate;Tp^{Me2} = hydrotris(3,5-dimethylpyrazolyl)borate; dppz = 3,5-diphenylpyrazolyl	

With the relatively longer lifetimes of **1** and **2** we were also interested to determine the photoluminescence quantum yields (PLQYs) of the compounds. The absolute quantum yields were measured using the Integrating Sphere method for **1** and **2** were 0.18 and 0.068 respectively (Figure S13-S14). As expected, the PLQY for **1** is higher than that of **2**. Further, the radiative (k_r) and non-radiative (k_{nr}) rates of **1** and **2** were calculated as 0.87×10^6 s^{-1}, 3.9×10^6 s^{-1} (k_r) and 0.47×10^6 s^{-1}, 6.38×10^6 s^{-1} (k_{nr}) respectively based on the quantum yields and lifetimes of these complexes, values that are comparable to reported cerium(III) emitters.[17]

Electrochemical measurements

Solution electrochemical studies have not previously been reported for complexes **1** and **2**. The cyclic voltammetry of these complexes was recorded in THF. For complex **1**, irreversible, anodic waves were observed at $E_{p,a}$ = −0.72 V and −0.51 V and an irreversible cathodic wave observed at $E_{p,c}$ = −2.56 V versus Fc/Fc^+(Figure 5). However, in contrast to the CV experiment for **1**, differential pulse voltammetry (DPV) studies revealed an approximately reversible process at $E_{1/2}$ = −0.80 V versus Fc/Fc^+ (Figure S16). The CV of complex **2** showed a quasi-reversible Ce(III/IV) redox couple at $E_{1/2}$ = −1.53 V and a second cathodic wave was observed at $E_{p,c}$ = −2.48 V versus Fc/Fc^+ (Figure 5, Figure S17, and Figure S18). The different anodic behaviour of **1** and **2** on electrochemical time scale indicates that chloride is more effectively stabilizing the Ce(IV)-containing product, resulting in the quasi-reversible wave observed in the CV of **2** at $E_{1/2}$ = −1.53 V. On the other hand, the triflate ligand evidently does not stabilize the Ce(IV)-containing product in the CV of **1** and two fully irreversible oxidation waves are observed for that complex.

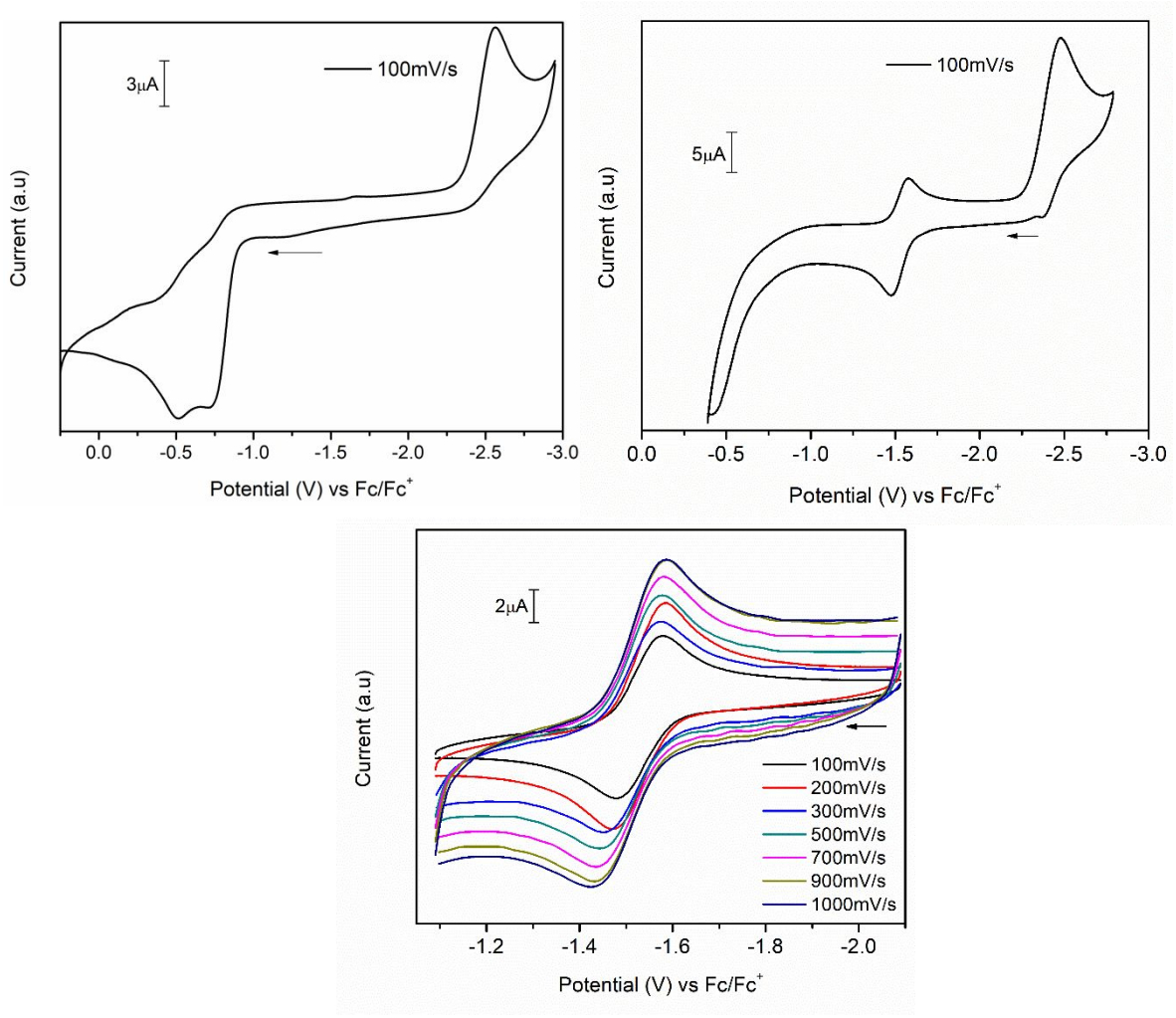

Figure 5. Cyclic voltammetry studies of **1** (full scan from 0.0 to –3.0 V) (left) and **2** (full scan from 0.0 to –3.0 V (right); Solvent: THF; electrolyte 0.1 M [^{n}Pr$_4$N][BAr$^{F}_4$]; [analyte] ~ 0.002 M ; v = 100 mV s^{-1}. Scan rate dependent study for **2** (below) with anodic scans started from –2.5 V.

With the ground state redox peak potentials ($E_{1/2}$) and emission band energies ($E_{0,0}$) in hand, we were also interested in calculating the excited state reduction potentials ($E_{1/2}$*) of **1** and **2** using the Rehm-Weller formalism: $E_{1/2}^{*} = E_{1/2} - E_{0,0} + \omega$.[17, 28, 29] The work function ω is typically considered a small contribution and was omitted here. In this way, the excited-state reduction potentials ($E_{1/2}$*) were estimated to be –3.31 and –4.02 V for complexes **1** and **2**, respectively (Table 3)

Table 3: Estimation of Ce$^{III/IV}$ reduction potential in the ^{2}D excited state for **1** and **2**.

Complex	$E_{1/2}$ (eV)	$E_{0,0}$ (eV)	$E_{1/2}$* (eV)
1	−0.80[a]	+2.51	−3.31
2	−1.53	+2.49	−4.02

[a] The DPV measurement was used to estimate the quasi-reversible $Ce^{III/IV}$ couple ($E_{1/2}$).

The very large negative estimated $E_{1/2}$* values place these Ce(III) complexes among the strongest photo-reductants reported to date.[16-18, 21] Both these complexes are more reducing than well-known photosensitizers of transition metals such as $[Ru(bpy)_3]^{2+}$ (bpy = 2,2′-bipyridine) ($E_{1/2}$* = −1.31 V versus Fc/Fc^+), *fac*-$Ir(ppy)_3$ (ppy =2,2′-phenylpyridine) ($E_{1/2}$* = −2.23 V versus Fc/Fc^+),[30] and $[(PNP)Cu^I]_2$ (PNP = bis(2-(diisobutylphosphino)phenyl)amide) ($E_{1/2}$* = −3.2 V versus Fc/Fc^+).[31] However, the $E_{1/2}$* of **1** could be considered as comparable to the previously reported, bench-stable photosensitizer, the hexachlorocerate(III) anion, $[Ce^{III}Cl_6]^{3-}$ with $E_{1/2}$* = −3.45 V versus Fc/Fc^+.[18]

Photochemical reactivity studies of 1 and 2

Complexes **1** and **2** absorb in the visible range and exhibit similar emission and excitation spectra with bright luminescence properties. With their relatively long excited state lifetimes, small Stokes shift values, sterically accessible coordination spheres, and large, negative excited state reduction potentials, **1** and **2** could be expected to be potent photo-reductants. To explore the efficacy of **1** and **2** as photo-reductants we were interested in exploring a halogen atom abstraction (XAT) reaction by activation of a C–X bond. Previously, our group had shown that Ce(III) complexes with similar photophysical properties induced dehalogenation (XAT) reactions.[16-18, 21] Inspired by those studies, complex **1** was tested for photoinduced XAT using benzyl chloride as a test substrate. In the absence of light, none of the expected benzyl radical homo-coupling product was observed after 24 h upon reaction with **1** (Scheme 3, Figure S20a). However, when complex **1** was allowed to react in sub-stoichiometric amount in the presence of light (467 nm) with 10 equiv benzyl chloride in THF-d_8 (0.6 mL) for 24 h at RT, a ^{1}H NMR spectrum of the reaction mixture showed formation of

bibenzyl with 70% yield based on the amount of **1**. Neutral COT, as indicated by a peak at 5.73 ppm, was also observed (Figure S19). Further, a control experiment indicated the benzyl chloride was stable and no bibenzyl product was observed in absence of complex **1** under 467 nm irradiation for 24 h at RT (Figure S20b).

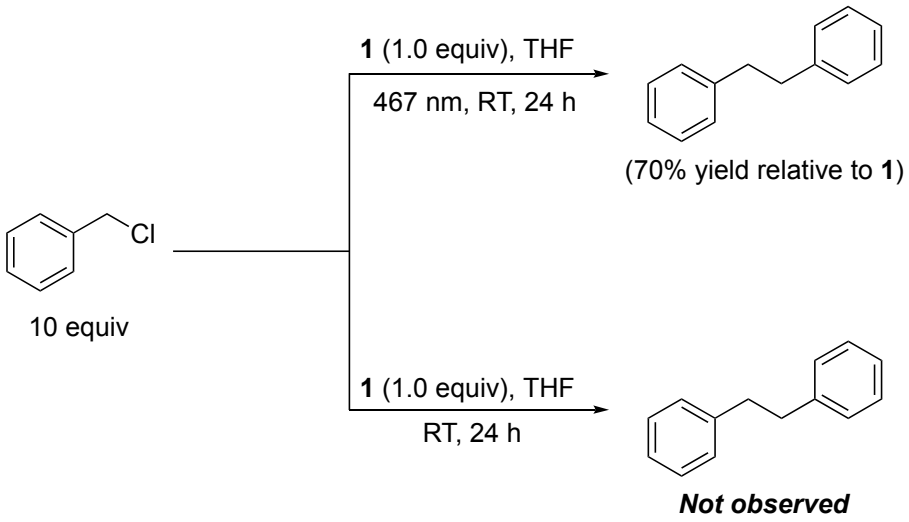

Scheme 3. XAT reaction of benzyl chloride in the presence of **1**.

This test reaction suggests that complex **1** induced halogen atom abstraction reaction with concomitant formation of bibenzyl and a cerium(IV) product. The low yield of bibenzyl and presence of neutral COT ligand in reaction mixture suggest that the cerium(IV) product decomposes to eliminate neutral COT. Well-defined cerium(IV) products (nor cerium(III) ones) were not identifiable nor isolable from these reaction mixtures. These results indicate a stoichiometric XAT reaction occurs upon photoirradiation of **1**, followed by degradation of the cerium(IV) products.

Similarly, complex **2** was also investigated for photoinduced XAT reaction of benzyl chloride under similar conditions. We expected that complex **2** with its highly reducing properties, based on its estimated $E_{1/2}^*$ value, relatively long excited state lifetime of τ = 145.8 $\pm$ 0.4 ns, and chloride ligands that could promote a more robust cerium(IV) structure upon oxidation, could similarly promote photo-reactivity. Indeed, in this case, reaction of **2** similarly resulted in the formation of bibenzyl product. However, due to low solubility of **2** in THF-d_8, quantification of the product formed was challenging in this case due to poor shimming from the presence of suspended solids (Figure S21). While bibenzyl product formation for **2** was similarly noted, along with neutral COT evident at 5.75 ppm in the ^{1}H NMR spectrum, the poor solubility

characteristics of **2** and presumed decomposition of **2** upon photo-oxidation indicate the potential for this photosensitizer to act catalytically is poor.

Conclusions

The organometallic *mono*(cyclooctatetraenide)Ce(III) complexes ($[(C_8H_8)Ce(\mu\text{-}X)(THF)_2]_2$, X = OTf^- (**1**), Cl^- (**2**), were studied for photophysical and photochemical reactivity. A new polymorph of the *mono*(cyclooctatetraenide)Ce(III) complex with triflate bridging ligands: $[(C_8H_8)Ce(\mu\text{-}O_3SCF_3)(THF)_2]_2$ (**1**) was synthesized and characterized, where the bridging triflate ligands assume a different geometry than previously observed. Complexes **1** and **2** showed characteristic emission and excitation bands in the visible region with bright green light emission under light irradiation. These complexes exhibit relatively long lifetimes and large, negative excited state reduction potentials ($E_{1/2}$*) with small Stokes shifts. Complexes **1** and **2** both display reactivity towards dehalogenation of the test substrate: benzyl chloride. Efforts are continuing to determine the metal-containing product of the XAT reaction and to further explore the potential for COT^{2-} complexes of cerium to act as photocatalysts.

EXPERIMENTAL SECTION

General Experimental Methods. For all reactions and manipulations performed under an inert atmosphere (N_2), standard Schlenk techniques or a Vacuum Atmospheres, Inc. Nexus II dry-box equipped with a molecular sieves 13X/Q5 Cu–0226S catalyst purifier system were used. Glassware was oven-dried overnight at 150 °C prior to use. ^{1}H NMR spectra were obtained on a Brüker UNI-400 Fourier transform NMR spectrometer at 400 MHz. ^{19}F NMR spectra was recorded on a Brüker UNI-400 Fourier transform NMR spectrometer at 376 MHz. All spectra were measured at 300 K unless otherwise specified. Chemical shifts were recorded in units of parts per million (ppm) downfield from residual proteo solvent peaks (^{1}H). An absolute referencing method was used in the Mnova software package for referencing the ^{19}F NMR spectra. FT-IR spectra were measured using KBr pellets on a Bruker Invenior R spectrometer. Elemental analyses were performed using a Costech ECS 4010 Analyzer.

Solvents. Tetrahydrofuran, toluene, hexanes were purchased from Fisher Scientific. The solvents were sparged for 20 min with dry N_2 and dried using a commercial solvent purification system comprising two columns of neutral alumina. Deuterated tetrahydrofuran and toluene were purchased from Cambridge Isotope Laboratories, Inc. both were dried using sodium ketyl and vacuum transferred before use.

Materials. Anhydrous $CeCl_3$ and $Ce(O_3SCF_3)_3$ were purchased from Strem Chemicals and used without further purification. Benzyl chloride was purchased from Aldrich and distilled under vacuum (to remove stabilizer), stored over 4 Å molecular sieves overnight before use. 1,3,5,7-Cyclooctatetraene (COT), 98%, stab. with 0.1% hydroquinone, was purchased from Thermo Scientific. COT was degassed by three freeze−pump−thaw cycles, stored in a greaseless Teflon sealable high vacuum flask inside the glovebox and passed through a short column of activated neutral alumina (to remove hydroquinone inhibitor) directly before use. K_2COT was freshly prepared in similar manner as reported in literature.[3] $CeCl_3(THF)_{1.5}$,[32] complexes **1** and **2** were prepared according to the reported procedures,[9, 11, 12] with slight modifications (see syntheses of **1** and **2** for details of modifications).

Electrochemistry. Voltammetry experiments (CV, DPV) were performed using a CH Instruments 620D Electrochemical Analyzer/Workstation and the data were processed using CHI software v9.24. All experiments were performed in an N_2 atmosphere dry-box using electrochemical cells that consisted of a 4 mL vial, glassy carbon working electrode, a platinum wire counter electrode, and a silver wire plated with AgCl as a quasi-reference electrode. The quasi-reference electrode was prepared by dipping a length of silver wire in concentrated hydrochloric acid. The working electrode surfaces were polished prior to each set of experiments. Potentials were reported versus ferrocene, which was added as an internal standard for calibration at the end of each run. Solutions employed during these studies were 2 mM in analyte and 100 mM in $[^nPr_4N][BArF_4]$ in 2 mL of tetrahydrofuran. All data were collected in a positive-feedback IR compensation mode.

Synthesis of $[(C_8H_8)Ce(\mu\text{-}O_3SCF_3)(THF)_2]_2$ (1).

In an N_2 filled glovebox, a 100 mL Schlenk flask with a Teflon coated stir bar was charged with $Ce(O_3SCF_3)_3$ (0.322 g, 0.55 mmol, 1 equiv) in 30 mL of THF. In a 20 mL scintillation vial, freshly prepared K_2COT (0.100 g, 0.55 mmol, 1 equiv) was dissolved

in 10 mL of THF and placed in a −20 °C freezer. After cooling the K_2COT solution for 30 min, the dark brown solution was added to the white suspension of $Ce(O_3SCF_3)_3$ dropwise. During the addition of the K_2COT solution, the colour of the reaction mixture changed from colourless to light brown to finally greenish yellow. The reaction mixture was allowed to stir for 48 h at RT. The volatile materials were then removed under reduced pressure. The resulting yellow solid was extracted with 20 mL cold THF and filtered through a pad of Celite on a medium porosity fritted filter. The solvent was stripped under reduced pressure to yield yellow solid **1**. X-ray quality crystals were obtained from concentrated THF solution of **1** layered with hexanes at –20° C. The greenish yellow crystals of **1** formed over 24 h and were then collected by filtration over a medium porosity fritted filter, washed with cold THF (1 × 2 mL) and RT hexanes (3 × 2 mL), and dried under reduced pressure to obtain **1**. Yield 0.340 g, 0.32 mmol, 58 %. ^{1}H NMR (400 MHz, THF-d_8) δ 3.63 (s, 16 H, THF), 2.92 (br, s,16 H, C_8H_8), 1.78 (s, 16 H, THF) ppm. ^{19}F NMR (376 MHz, THF-d_8) δ –77.92 ppm. FT-IR (cm^{-1}): 3045 (m), 3022 (m), 2982 (m), 2889 (m), 2137 (m), 1740 (w), 1460 (w), 1309 (m), 1244 (s), 1230 (s), 1097 (w), 1034 (s), 913 (w), 873 (s), 767 (m), 706 (s), 638 (s), 579 (m), 518 (s).

Synthesis of $[(C_8H_8)Ce(\mu\text{-}Cl)(THF)_2]_2$ (2).

In an N_2 filled glovebox, a 100 mL Schlenk flask with a Teflon coated stir bar was charged with $CeCl_3(THF)_{1.5}$ (0.195 g, 0.55 mmol, 1 equiv) in 40 mL of THF. In a 20 mL scintillation vial, freshly prepared K_2COT (0.100 g, 0.55 mmol, 1 equiv) was dissolved in 10 mL of THF and the solution was placed in a −20 °C freezer. After cooling for 30 min, the dark brown solution of K_2COT was added to the white suspension of $CeCl_3(THF)_{1.5}$ dropwise. During the addition of the K_2COT solution, the colour of the reaction mixture changed from colourless to light green followed by bright yellow. The reaction mixture was allowed to stir for 48 h at RT. Afterwards the reaction mixture was filtered through a pad of Celite on a medium porosity fritted filter. The solvent was stripped under reduced pressure to yield a yellow solid. To remove the more soluble side product ($K[Ce(COT)_2]$), the crude yellow solid was washed with cold THF (3 × 3 mL) . The remaining bright yellow solid was extracted with hot THF and the saturated solution was kept at –20° C to give **2**. X-ray quality crystals were obtained from a concentrated THF solution of **2** at –20° C. The yellow crystals, that formed over a period of 24 h, were collected by filtration over a medium porosity fritted filter, washed

with cold THF (1 × 2 mL) and RT hexanes (3 × 2 mL) and dried under reduced pressure to obtain **2**. Yield 0.243 g, 0.29 mmol, 52 %.^{1}H NMR (400 MHz, THF-d_8) δ 3.62 (s, 16 H, THF), 1.77 (s, 16 H, THF), 1.29 (s,16 H, C_8H_8), ppm. FT-IR (cm^{-1}): 1091 (w) 1015 (s) 927 (w, sh) 796 (w) 739 (w) 887 (s) 693 (vs)

General procedures for the photo-reactivity studies of 1 and 2.

Inside the glovebox, in an air tight vial with screw cap, *mono*(cyclooctatetraenyl)-Ce(III) complex **1** or **2** was suspended with 0.6 mL of THF-d_8 and a Teflon stir bar. To the greenish yellow solution (or suspension), 10 equiv benzyl chloride was added. The vial was then sealed and removed from the glovebox. The reaction mixture was stirred for 24 h and irradiated with 467 nm visible light at RT using a Kessel lamp (467 nm PRL160 Kessel lamp) at a distance of 3.0 cm. Afterwards the vial with reaction mixture was transferred back into the glovebox and transferred to an NMR tube. An ^{1}H NMR of the reaction mixture was then recorded to observe the product formation, where the amount of product formed was measured relative to benzyl chloride by integrating the area under the characteristic peaks at 4.6 ppm and 2.9 ppm for benzyl chloride and bibenzyl respectively. Due to low solubility of **2** in THF-d_8 and the presence of suspended solids, quantification of the product formation was difficult as shimming of NMR sample was poor.

Acknowledgment

We gratefully acknowledge the Office of Basic Energy Sciences, Chemical Sciences, Geosciences and Biosciences Division, Materials and Chemical Sciences Research for Quantum Information Science Program, of the U.S. Department of Energy under Award DE-SC0020169 for support of this work. We also thank Prof. Neil C. Tomson for use of his UV-Vis-NIR instrument. E.J.S. also thanks the University of Pennsylvania for financial support. We also thank the JASCO Center at the University of Pennsylvania for providing access to JASCO spectrofluorometer FP-8300 with ILF-835 100 mm diameter Integrating Sphere system.

References

1. F. M. Sroor, *J. Organomet. Chem.*, 2021, **948**.
2. J. Greenough, Z. Zhou, Z. Wei and M. A. Petrukhina, *Dalton Trans*, 2019, **48**, 5614-5620.
3. A. Streitwieser, Jr. and U. Mueller-Westerhoff, *J. Am. Chem. Soc.*, 1968, **90**, 7364-7364.
4. A. Zalkin and K. N. Raymond, *J. Am. Chem. Soc.*, 1969, **91**, 5667-5668.

5. D. E. Smiles, E. R. Batista, C. H. Booth, D. L. Clark, J. M. Keith, S. A. Kozimor, R. L. Martin, S. G. Minasian, D. K. Shuh, S. C. E. Stieber and T. Tyliszczak, *Chemical Science*, 2020, **11**, 2796-2809.
6. J. J. Le Roy, L. Ungur, I. Korobkov, L. F. Chibotaru and M. Murugesu, *J. Am. Chem. Soc.*, 2014, **136**, 8003-8010.
7. D.-C. Sergentu, C. H. Booth and J. Autschbach, *Chemistry – A European Journal*, 2021, **27**, 7239-7251.
8. C. H. Booth, M. D. Walter, M. Daniel, W. W. Lukens and R. A. Andersen, *Phys. Rev. Lett.*, 2005, **95**, 267202.
9. K. O. Hodgson and K. N. Raymond, *Inorg. Chem.*, 1972, **11**, 171-175.
10. K. O. Hodgson, F. Mares, D. Starks and A. Streitwieser, *J. Am. Chem. Soc.*, 1973, **95**, 8650-8658.
11. F. Mares, K. O. Hodgson and A. Streitwieser, *J. Organomet. Chem.*, 1971, **28**, C24-C26.
12. U. Kilimann, M. Schäfer, R. Herbst-Irmer and F. T. Edelmann, *J. Organomet. Chem.*, 1994, **469**, C10-C14.
13. O. S. Wenger, *J. Am. Chem. Soc.*, 2018, **140**, 13522-13533.
14. P. N. Hazin, J. W. Bruno and H. G. Brittain, *Organometallics*, 1987, **6**, 913-918.
15. M. Suta, N. Harmgarth, M. Kühling, P. Liebing, F. T. Edelmann and C. Wickleder, *Chemistry – An Asian Journal*, 2018, **13**, 1038-1044.
16. H. Yin, P. J. Carroll, J. M. Anna and E. J. Schelter, *J. Am. Chem. Soc.*, 2015, **137**, 9234-9237.
17. H. Yin, P. J. Carroll, B. C. Manor, J. M. Anna and E. J. Schelter, *J. Am. Chem. Soc.*, 2016, **138**, 5984-5993.
18. H. Yin, Y. Jin, J. E. Hertzog, K. C. Mullane, P. J. Carroll, B. C. Manor, J. M. Anna and E. J. Schelter, *J. Am. Chem. Soc.*, 2016, **138**, 16266-16273.
19. Y. Qiao, D.-C. Sergentu, H. Yin, A. V. Zabula, T. Cheisson, A. McSkimming, B. C. Manor, P. J. Carroll, J. M. Anna, J. Autschbach and E. J. Schelter, *J. Am. Chem. Soc.*, 2018, **140**, 4588-4595.
20. Y. Qiao, Q. Yang and E. J. Schelter, *Angew. Chem. Int. Ed.*, 2018, **57**, 10999-11003.
21. Y. Qiao, T. Cheisson, B. C. Manor, P. J. Carroll and E. J. Schelter, *Chem Commun (Camb)*, 2019, **55**, 4067-4070.
22. Q. Yang, Y.-H. Wang, Y. Qiao, M. Gau, P. J. Carroll, P. J. Walsh and E. J. Schelter, *Science*, 2021, **372**, 847-852.
23. U. Reißmann, P. Poremba, M. Noltemeyer, H.-G. Schmidt and F. T. Edelmann, *Inorg. Chim. Acta*, 2000, **303**, 156-162.
24. W. Yan, Z. Cai, H. Qi, R. Guo, Z. Liu and Z. Bian, *Dalton Trans*, 2022, **51**, 3234-3240.
25. W. Yan, L. Wang, H. Qi, G. Zhan, P. Fang, Z. Liu and Z. Bian, *Inorg. Chem.*, 2021, **60**, 18103-18111.
26. X.-L. Zheng, Y. Liu, M. Pan, X.-Q. Lü, J.-Y. Zhang, C.-Y. Zhao, Y.-X. Tong and C.-Y. Su, *Angew. Chem. Int. Ed.*, 2007, **46**, 7399-7403.
27. Z. Zhao, L. Wang, G. Zhan, Z. Liu, Z. Bian and C. Huang, *National Science Review*, 2021, **8**, nwaa193.
28. D. Rehm and A. Weller, *Isr. J. Chem.*, 1970, **8**, 259-271.
29. J. W. Tucker and C. R. J. Stephenson, *The Journal of Organic Chemistry*, 2012, **77**, 1617-1622.
30. T. Koike and M. Akita, *Inorganic Chemistry Frontiers*, 2014, **1**, 562-576.
31. S. B. Harkins and J. C. Peters, *J. Am. Chem. Soc.*, 2005, **127**, 2030-2031.
32. H. J. Heeres, J. Renkema, M. Booij, A. Meetsma and J. H. Teuben, *Organometallics*, 1988, **7**, 2495-2502.